© 2017. Published by The Company of Biologists Ltd | Development (2017) 144, 2009-2020 doi:10.1242/dev.146332

RESEARCH ARTICLE

Lmx1b-targeted *cis*-regulatory modules involved in limb dorsalization

Endika Haro[1], Billy A. Watson[1,2], Jennifer M. Feenstra[1], Luke Tegeler[1], Charmaine U. Pira[1], Subburaman Mohan[3] and Kerby C. Oberg[1,*]

ABSTRACT

Lmx1b is a homeodomain transcription factor responsible for limb dorsalization. Despite striking double-ventral (loss-of-function) and double-dorsal (gain-of-function) limb phenotypes, no direct gene targets in the limb have been confirmed. To determine direct targets, we performed a chromatin immunoprecipitation against Lmx1b in mouse limbs at embryonic day 12.5 followed by next-generation sequencing (ChIP-seq). Nearly 84% (*n*=617) of the Lmx1b-bound genomic intervals (LBIs) identified overlap with chromatin regulatory marks indicative of potential *cis*-regulatory modules (PCRMs). In addition, 73 LBIs mapped to CRMs that are known to be active during limb development. We compared Lmx1b-bound PCRMs with genes regulated by Lmx1b and found 292 PCRMs within 1 Mb of 254 Lmx1b-regulated genes. Gene ontological analysis suggests that Lmx1b targets extracellular matrix production, bone/joint formation, axonal guidance, vascular development, cell proliferation and cell movement. We validated the functional activity of a PCRM associated with joint-related *Gdf5* that provides a mechanism for Lmx1b-mediated joint modification and a PCRM associated with *Lmx1b* that suggests a role in autoregulation. This is the first report to describe genome-wide Lmx1b binding during limb development, directly linking Lmx1b to targets that accomplish limb dorsalization.

KEY WORDS: Lmx1b, Dorsal-ventral patterning, Enhancer, Limb, Dorsalization, Mouse

INTRODUCTION

The presence of morphologically distinguishable dorsal and ventral limb asymmetry reflects the polarized pattern accomplished during development. In mouse limbs, hair only appears on the dorsal surface of the autopod and nails on the dorsal aspect of digit tips, whereas footpads and ecrine glands are restricted ventrally. Internal differences are also present. Muscles develop as dorsal extensors and ventral flexors with disparate attachments, bones show subtle asymmetry, and joint morphology supports ventral flexion.

The polarity of the limb ectoderm is achieved by the restricted expression domains of wingless-type MMTV integration site family member 7a (*Wnt7a*) and engrailed 1 (*En1*) (Parr and McMahon, 1995; Loomis et al., 1996; Cygan et al., 1997; Loomis et al., 1998). As the limb begins to emerge, *Wnt7a* expression wraps around the limb bud apex (Bell et al., 1998). Bmp signals from the lateral plate mesoderm trigger the activation of *En1* in the ventral limb ectoderm (Pizette et al., 2001). *En1* expression expands in the ventral ectoderm, restricting *Wnt7a* expression to the dorsal ectoderm (Loomis et al., 1996; Cygan et al., 1997; Loomis et al., 1998). The restricted dorsal secretion of Wnt7a imparts polarity to the underlying limb mesoderm by triggering the expression of Lmx1b, a LIM homeodomain transcription factor that is ultimately responsible for limb dorsalization (Chen et al., 1998; Parr and McMahon, 1995; Riddle et al., 1995; Vogel et al., 1995). Mice lacking functional Lmx1b develop a ventral-ventral limb phenotype, whereas ectopic ventral expression of Lmx1b leads to a dorsal-dorsal limb phenotype (Chen et al., 1998; Cygan et al., 1997; Vogel et al., 1995). In humans, haploinsufficiency of *LMX1B* is associated with nail-patella syndrome, which is characterized by nail dysplasia, absent or hypoplastic patellae, progressive renal disease and decreased bone mineral density (Chen et al., 1998; Towers et al., 2005; Dreyer et al., 2000).

Despite the striking effect of Lmx1b on dorsal limb morphology, direct targets in the limb have been elusive. A number of potential targets have been suggested by comparative gene arrays between wild-type and *Lmx1b* knockout mice, but none has been confirmed (Feenstra et al., 2012; Gu and Kania, 2010; Krawchuk and Kania, 2008). Therefore, in order to elucidate direct limb targets for Lmx1b, we performed chromatin immunoprecipitation against Lmx1b followed by massive parallel sequencing (ChIP-seq) of mouse limbs during dorsalization [embryonic day (E) 12.5] and compared these sites of Lmx1b binding with genes regulated by Lmx1b. In this article, we describe the identification of Lmx1b-bound potential *cis*-regulatory modules (PCRMs) associated with Lmx1b-regulated genes and the predicted functional pathways affected. These data suggest that Lmx1b exerts its dorsalizing effects through the targeted regulation of genes involved in bone/joint development, extracellular matrix composition, axon tracking and cell proliferation. Intriguingly, we also identified an Lmx1b-bound PCRM upstream of the *Lmx1b* gene that provides the capacity for autoregulation.

RESULTS

Validation and genome-wide characterization of the Lmx1b ChIP-seq

Feenstra and co-workers (Feenstra et al., 2012) found more limb bud genes differentially expressed in the presence of Lmx1b at E12.5 than at either E11.5 or E13.5. Therefore, we performed ChIP-seq analyses on E12.5 mouse limbs. After peak calling analysis (MACS algorithm v1.4.2, cutoff P<1e-5), we identified 735 Lmx1b-bound genomic fragments or intervals (LBIs) common to ChIP-seq replicates with an average length of 470 bp (Table S1).

Comparison of LBIs with the annotated mouse genome showed that intronic (36%) or intergenic (54%) regions were the most

[1]Department of Pathology and Human Anatomy, Loma Linda University, Loma Linda, CA 92354, USA. [2]Department of Basic Sciences, Loma Linda University, Loma Linda, CA 92354, USA. [3]Musculoskeletal Disease Center, Loma Linda VA HealthCare System, Loma Linda, CA 92357, USA.

*Author for correspondence (koberg@llu.edu)

K.C.O., 0000-0002-1241-4273

Received 9 December 2016; Accepted 17 April 2017

Development (2017) 144, 2009-2020 doi:10.1242/dev.146332

common sites for Lmx1b binding (Fig. 1A). Of the regions mapped, 1% were within coding regions, 2% were found within the 5′UTR and 1% within the 3′UTR. Finally, only 6% of the intervals localized to potential promoters [−2500 and +500 bp from the transcription start sites (TSSs) based on UCSC gene annotation].

MEME-ChIP (Bailey et al., 2015) analysis for *de novo* motif discovery retrieved TMATWA (M=C or A, W=T or A) as the most common motif found in the Lmx1b-bound genomic regions (*P*=3.5e-29) (Fig. 1B). The TMATWA motif includes the published Lmx1b-binding site (TAATTA) (Morello et al., 2001) and the distribution of both motifs within intervals was similar (*P*=4.5e-24), consistent with Lmx1b as the ChIPed transcription factor.

The biological functions of promoter-associated intervals were predominantly related to genes with general cell functions as determined by GREAT analysis (Fig. 1C) (McLean et al., 2010). The intronic-associated intervals correlated with genes involved in growth and organ development, including limb

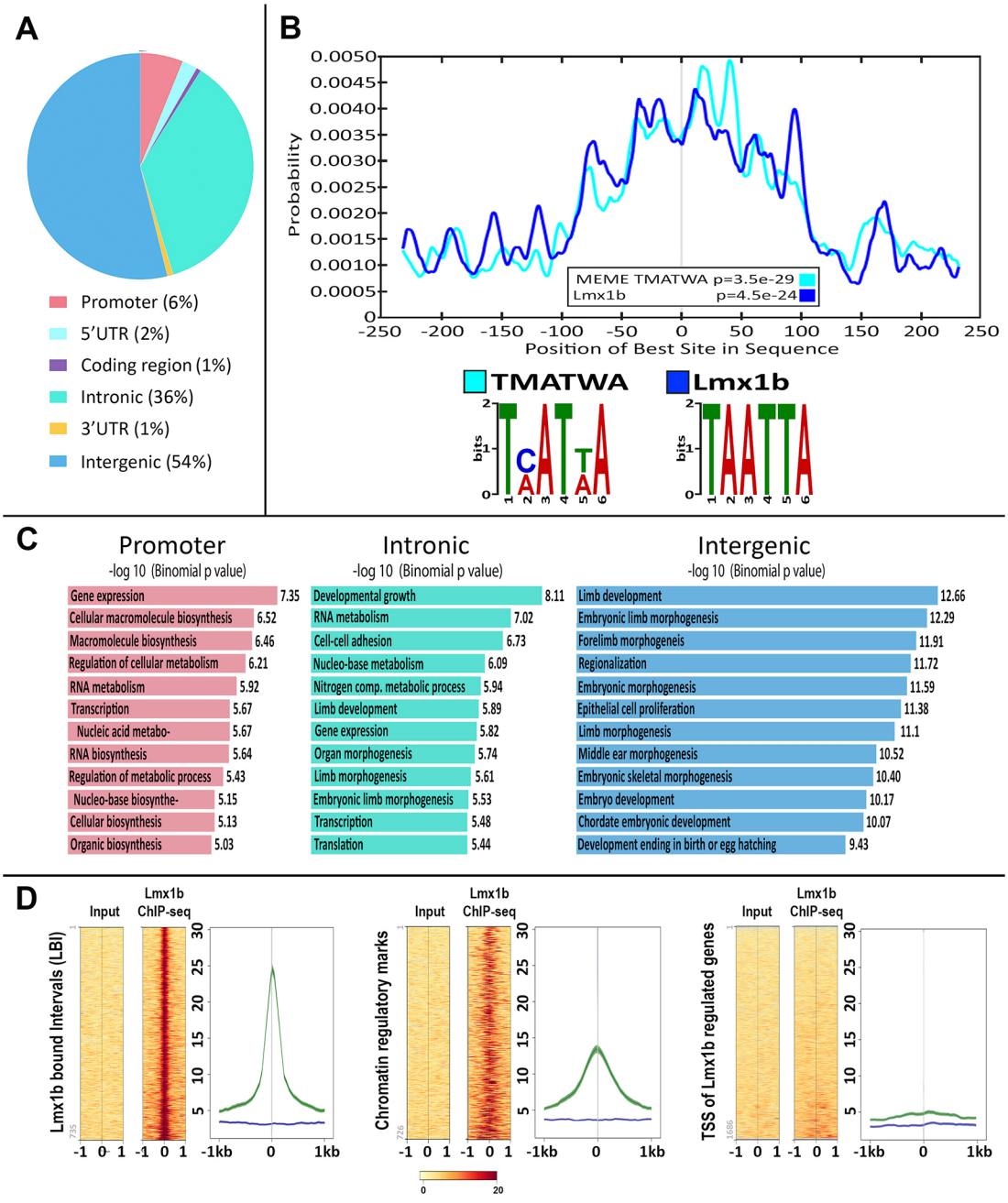

Fig. 1. Validation and characterization of Lmx1b-bound intervals. (A) Genome-wide distribution of LBIs showing a high percentage of intervals in intergenic and intronic regions. (B) Distribution of the *de novo* identified Lmx1b-ChIPed motif (TMATWA) and predicted distribution of the published TAATTA binding motif (Morello et al., 2001) for Lmx1b in the intervals retrieved from ChIP-seq experiments. (C) GREAT analysis of annotated genes within 1 Mb of LBIs showing limb development-related genes associated with intergenic and intronic intervals. (D) Heatmaps (left) and summarized averages plots (right) for input and Lmx1b-ChIPed DNA according to fraction of reads aligned to Lmx1b-bound intervals (left panel); genomic regions associated with *cis*-regulatory activity (H3K27ac, H3K4me2, p300, RNAP2 and/or Med12) that overlapped Lmx1b-targeted intervals (Visel et al., 2009; Berlivet et al., 2013; Cotney et al., 2013; DeMare et al., 2013) (middle); and TSS of Lmxb1-regulated genes (right). Lmx1b preferentially binds to regulatory regions rather than promoters.

Development (2017) 144, 2009-2020 doi:10.1242/dev.146332

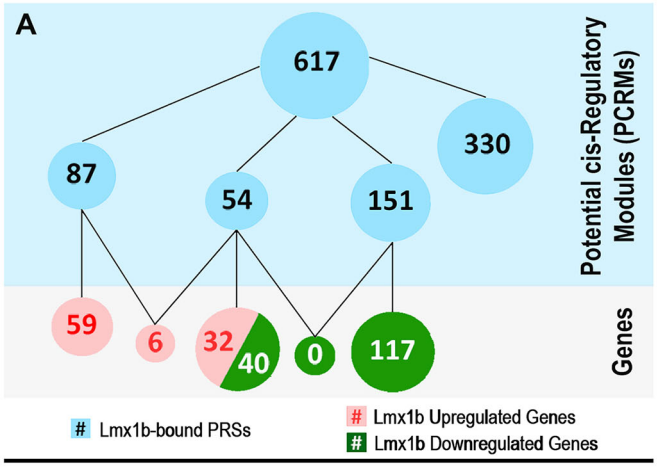

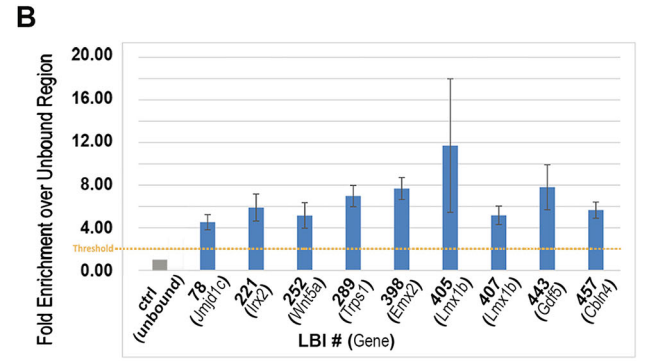

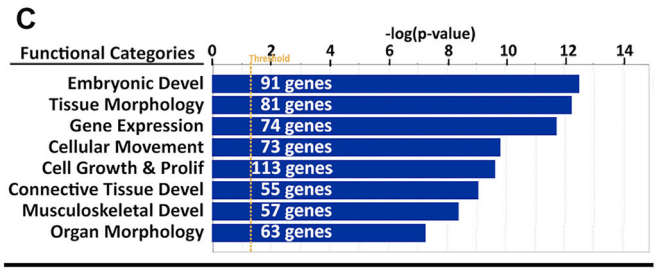

D

Annotated Functions	
Limb Development	17
Forelimb	3
Hindlimb	5
Limb Morphogenesis	36
Size/Length	18
Stylopod	8
Zeugopod	10
Tissue Development	62
Connective Tissue	37
Cartilage	16
Bone	23
Muscle	37
Cell Development	121
Connective Tissue	118
Cartilage	17
bone	25

Limb Development	
Genes	Fold Change
Lmx1b	5.685
Hapln1	2.399
Alx1	2.343
Gdf5	2.098
Pthlh	1.831
Prkg2	1.558
Fgf8	1.506
Fgfr3	1.497
Osr2	1.456
Comp	1.449
Shox2	1.426
Med1	1.402
Hgf	-1.439
Ror2	-1.525
Wnt5a	-1.530
Nr2f2	-1.638
Col1a2	-1.684

Fig. 2. Functional categories of PCRM-associated Lmx1b-regulated genes. (A) Bubble diagram depicting the associations between Lmx1b-bound PCRMs (blue) and genes differentially regulated in the presence of Lmx1b: upregulated (red) and downregulated (green). More than one PCRM can associate with a gene and more than one gene can associate with a PCRM. (B) Enrichment of Lmx1b-bound PCRMs by ChIP-qPCR is indicated as fold change of % input over the unbound control (for tested LBIs, $P<0.001$, $n=6$). Associated genes are shown in parentheses for each LBI. (C) Predicted functional categories of PCRM-associated Lmx1b-regulated genes using Ingenuity Pathway Analysis (Table S4). (D) Annotated functions within the functional categories listed in C. The numbers of affected Lmx1b-bound genes are listed on the left (Table S4). The associated genes for the limb development category are listed on the right in the shaded box. Note: a gene can be classified in more than one functional category.

morphogenesis. Remarkably, the intergenic-associated genomic regions were enriched near genes related to limb and skeletal development, which are functions that are anticipated to be modified by Lmx1b.

Lmx1b binding is associated with active regulation

Although the annotated location and GREAT analysis give some insight into the potential regulatory activity of the LBIs, *cis*-regulatory modules (CRMs) are characterized by histone-modifying co-factors and bound proteins, collectively called chromatin regulatory marks, that affect genome accessibility (Hardison and Taylor, 2012). p300 (Ep300 – Mouse Genome Informatics) is a ubiquitous phosphoprotein with intrinsic histone acetyltransferase activity that predicts regulatory activity in a tissue-specific manner (Visel et al., 2009). Because *Lmx1b* is also expressed in other tissues, including forebrain, midbrain, hindbrain, spinal cord, kidney and the eye (Chen et al., 1998; Asbreuk et al., 2002), we evaluated whether the distribution of the 735 LBIs conformed to a limb-specific pattern. We compared the 735 LBIs with p300 ChIP-seq data in available embryonic tissues, i.e. limb, forebrain and midbrain (Visel et al., 2009), and confirmed that more LBIs colocalized with p300 from the limb (288, ∼39%), than from either the forebrain (25, ∼3%) or midbrain (1, ∼0.1%) (Fig. S1A), consistent with a limb-specific pattern of regulatory activity.

Overlap of an LBI with multiple chromatin regulatory marks increases confidence in its role as a regulatory sequence (Hardison and Taylor, 2012). Thus, in addition to p300, we compared the LBIs with available ChIP-seq data for chromatin regulatory marks associated with enhancer elements (H3K27ac and H3K4me2) (Heintzman et al., 2009) and regulatory regions undergoing active transcription (RNAP2 and Med12) (Kagey et al., 2010) in E12.5 and E11.5 limbs. We recognize that regulation during these stages is dynamic and what is active at E11.5 might not be active at E12.5; however, these data would still highlight a PCRM. After peak calling analyses, the Lmx1b ChIP-seq reads exhibited a 7-fold enrichment in tagged sequences within the 735 LBIs when compared with the input DNA (Fig. 1D). We next analyzed the distribution of tagged sequences within LBIs that overlap chromatin regulatory marks. We found that Lmx1b-ChIPed DNA was enriched within enhancer-associated chromatin marks (H3K27ac and H3K4me2) and exhibited a 3-fold enrichment over input DNA, whereas the enrichment within actively transcribed regulatory regions was 5-fold (RNAP2 and Med12) (Fig. S1B). Overall, Lmx1b ChIP-seq DNA sequences show a 4-fold enrichment within chromatin regulatory marks, consistent with a role for Lmx1b as a factor involved in active regulation (Fig. 1D; Fig. S3). As both CRMs and promoters are active regulatory regions, we examined the TSSs for genes regulated by Lmx1b (Feenstra et al., 2012). Similar to the genomic distribution of LBIs, no TSS enrichment was found in the distribution of tagged sequences between Lmx1b-ChIPed DNA and input DNA (Fig. 1D) supporting the concept that Lmx1b-mediated regulation favors CRMs over promoters.

We required at least two active regulatory marks for an interval to be categorized as a PCRM. Based on this criterion, we determined

Development (2017) 144, 2009-2020 doi:10.1242/dev.146332

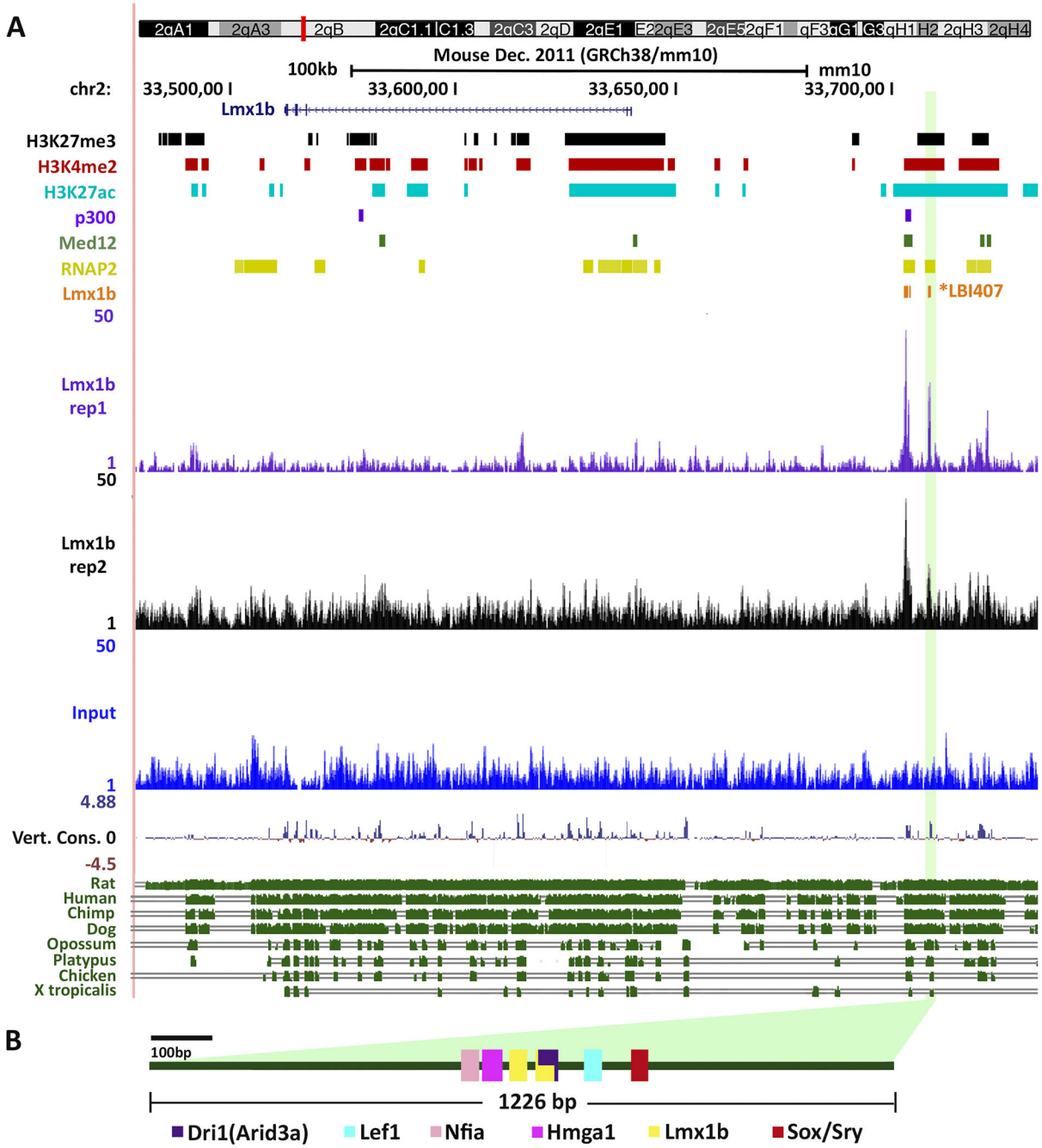

Fig. 3. LBI407 is a highly conserved PCRM upstream of *Lmx1b*. (A) Annotated browser image depicting chromosomal location of LBI407, 66 kb upstream of *Lmx1b*. Chromatin-associated marks (Visel et al., 2009; Berlivet et al., 2013; Cotney et al., 2013; DeMare et al., 2013), location of intervals bound by the transcription factor Lmx1b in E12.5 mouse limbs, and conservation obtained from the UCSC genome browser are shown (top to bottom). LBI407 (highlighted by a vertical green shaded bar) is highly conserved across vertebrate species and overlaps with four chromatin-associated marks (both active and repressor). (B) *In silico* analysis of potential transcription factor-binding sites within LBI407 exhibiting two potential binding sites for Lmx1b (yellow).

that 617 of the 735 LBIs were PCRMs (Fig. 2A; Table S2). The number of PCRMs was 30 times higher than random genomic regions with comparable characteristics (n=5 groups, each with 735 random genomic intervals; one-sample t-test P<1e-4) (Fig. S2A). The PCRMs were dispersed throughout the genome with the largest number (51) being found in chromosome 1, the largest chromosome. Interestingly, no PCRMs were identified in the X chromosome, although it is nearly as large as chromosome 2 and 28 Lmx1b-regulated genes are found on the X chromosome (Fig. S3). LBIs that overlapped repressive regulatory marks (H3K27me3) were found in 50 intervals, 41 of which were also associated with two or more active regulatory marks (Table S2). Intervals associated with repressive regulatory marks alone or with fewer than two active regulatory marks (n=9) were considered inactive PCRMs or nonspecific Lmx1b binding (Table S2).

Lmx1b-bound PCRMs are associated with Lmx1b-regulated genes

In order to determine direct limb targets, we compared Lmx1b-bound PCRMs with genes previously reported to be regulated by

Development (2017) 144, 2009-2020 doi:10.1242/dev.146332

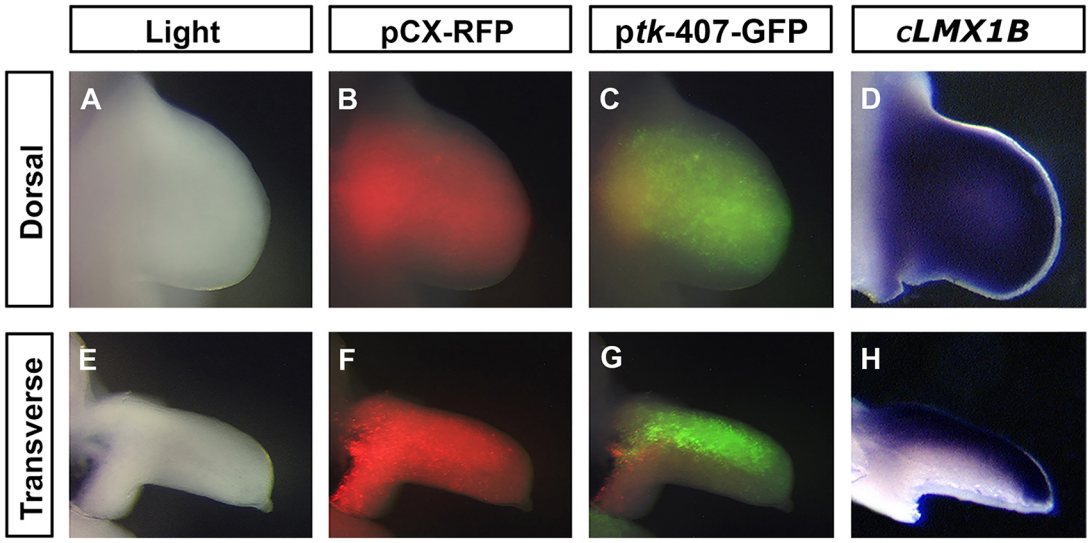

Fig. 4. LBI407 is a dorsally restricted enhancer coincident with *LMX1B* expression. (A-H) Dorsal (A-C) and transverse (E-G) views of chicken wing buds 48 h after electroporation at HH14, and *in situ* hybridization for *LMX1B* in HH24 chicken wing buds (D,H). Transfection efficiency is determined by β-actin promoter-driven RFP (B,F). Enhancer activity of LBI407 drives GFP expression in the dorsal limb mesoderm (C,G) coincident with the pattern of *LMX1B* expression (D,H). The dorsal and transverse fluorescence views are overlaid with light field to define limb boundaries.

Lmx1b at E12.5 (Feenstra et al., 2012). We found 292 PCRMs within 1 Mb of 254 Lmx1b-regulated genes (Fig. 2A; Table S3). In contrast, when we compared random non-Lmx1b-bound regulatory sequences (n=5 groups, each with 292 H3K27ac -positive intervals) with the 254 Lmx1b-regulated genes, only 60 (s.d.=7) regulatory sequences on average associated with 75 (s.d.=11) genes. This indicates that Lmx1b-PCRMs are enriched for their associated gene targets 5-fold over random regulatory sequences (one-sample t-test analysis, P<1e-4) (Fig. S2B). We also found that some PCRMs were associated with more than one gene and some genes were associated with multiple PCRMs (Fig. 2A). Enrichment of Lmx1b-bound gene-associated PCRMs was validated by qPCR using two independently generated ChIP samples. Nine PCRMs were selected and each exhibited at least a 4-fold enrichment when compared with an unbound control region (Fig. 2B).

Ingenuity Pathway Analysis (IPA) of the 254 genes associated with PCRMs demonstrated a significant effect on eight functional categories relevant to limb development. These categories include connective tissue development/function, skeletal and muscle system development/function and cellular movement, with some genes present in more than one functional category (Fig. 2C; Table S4). Within the functional categories affected, genes were further subcategorized into limb-related annotated functions (Fig. 2D; Table S4) including 17 that mapped to the annotated biological process termed ‘limb development’. IPA analyses also predicted that canonical pathways involved in movement, proliferation, cell adhesion, cytoskeletal regulation, and vascular development were targeted (Fig. S4).

Within the connective tissue development category, we found several genes involved with extracellular matrix (ECM) composition that are associated with Lmx1b-bound PCRMs including *Col1a2*, *Col11a2*, *Kera*, *Lum*, *Dcn*, *Matn1/4*, *Epyc* and *Has3* (Table S4). In addition, a number of genes associated with bone/joint differentiation, *Osr2*, *Gdf5*, *Runx2*, *Sox11* and *Trps1* (Table S4), were present within the skeletal and muscle systems development/function category.

PCRMs associated with Lmx1b-regulated genes are active during limb development

We performed comparative analyses using the VISTA browser (Frazer et al., 2004) to identify conserved PCRMs that were more likely to be functional across species. A high degree of conservation (greater than 70% homology) was found in 289 LBIs. Approximately 90% of the conserved LBIs are PCRMs with 105 associated with 94 Lmx1b-regulated genes (Tables S2 and S3).

Further functional validation was performed on two conserved Lmx1b-bound PCRMs. One of the PCRMs (LBI407) is 66 kb upstream of *Lmx1b* on murine chromosome 2 (Fig. 3A; Table S3). *In silico* analysis for transcription factor-binding sites in LBI407 confirmed two potential sites for Lmx1b as well as several other transcription factors (Fig. 3B). LBI407 (1224 bp) was isolated from murine genomic DNA, linked to a GFP reporter and transfected into chick presumptive limb mesoderm by electroporation. LBI407 showed robust enhancer activity in the limb 48 h after transfection (Fig. 4A-C,E-G). Moreover, its activity was restricted to the dorsal mesoderm coincident with *LMX1B* expression (Fig. 4D,H) (Vogel et al., 1995; Riddle et al., 1995; Dreyer et al., 2000).

We validated the activity of another PCRM (LBI443 from Table S3) located 82 kb downstream of growth differentiation factor 5 (*Gdf5*) (Fig. 5A), a factor known to be involved in joint development (Settle et al., 2003). This PCRM contained multiple potential binding sites for Lmx1b, Sox and Osr2 transcription factors (Fig. 5B). A GFP reporter construct containing the LBI443 (867 bp) isolated from murine DNA was transfected into chick presumptive limb mesoderm. LBI443 exhibited enhancer activity in the elbow, wrist, and digit joints overlapping *GDF5* expression (Fig. 6C-C″). Furthermore, using section *in situ* hybridization we demonstrate that *LMX1B* expression overlaps both LBI443 activity and *GDF5* expression (Fig. 6E-G′) dorsally in the developing elbow joint, consistent with a role for LMX1B-mediated dorsalization.

An additional 91 Lmx1b-bound PCRMs correspond to previously published conserved non-coding DNA sequences

Development (2017) 144, 2009-2020 doi:10.1242/dev.146332

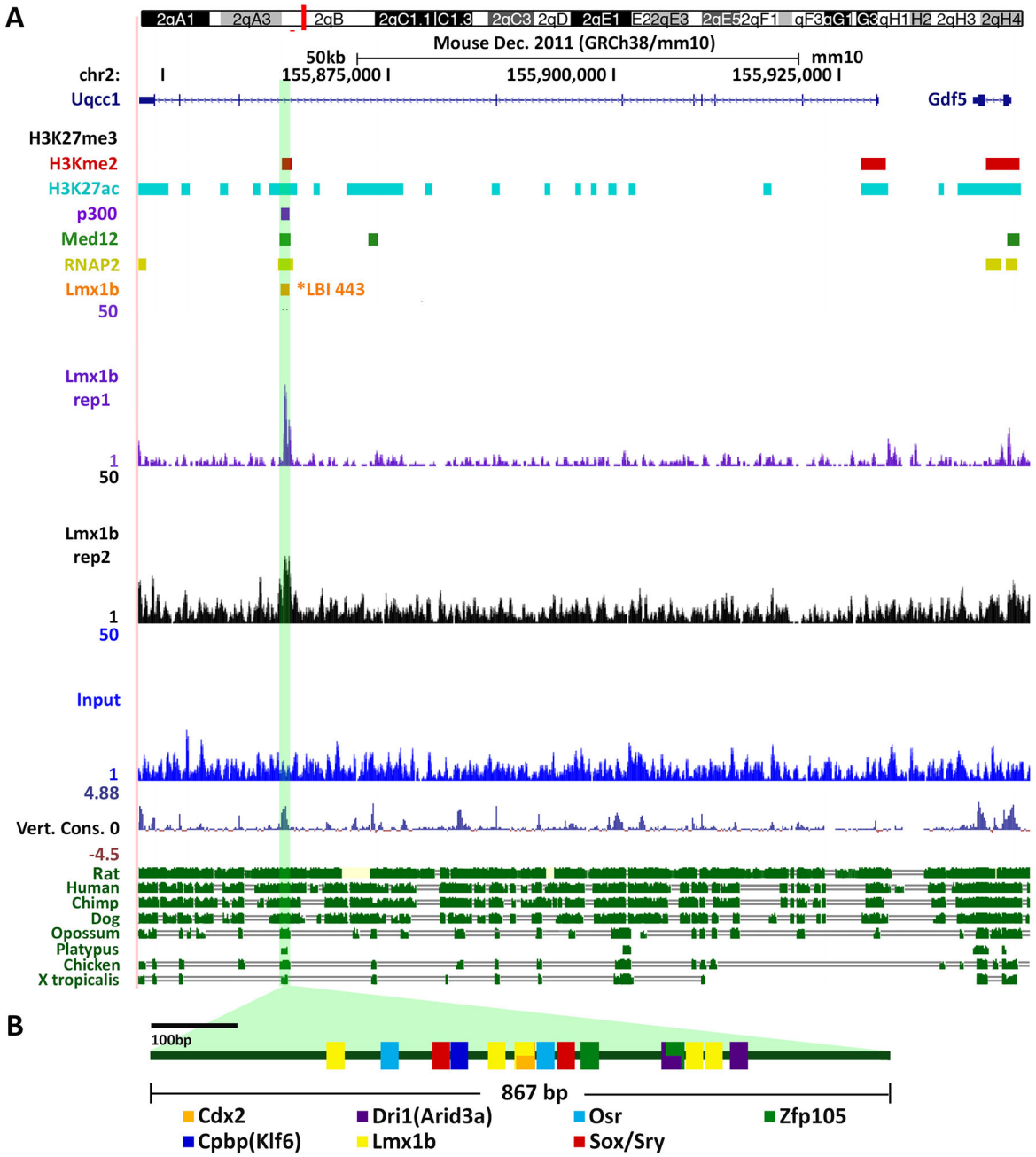

Fig. 5. LBI443 is a highly conserved PCRM downstream of *Gdf5*. (A) Annotated browser image depicting chromosomal location of LBI443, 82 kb downstream of *Gdf5*. Chromatin-associated marks (Visel et al., 2009; Berlivet et al., 2013; Cotney et al., 2013; DeMare et al., 2013), Lmx1b-bound interval from E12.5 mouse limbs, and conservation obtained from the UCSC genome browser are shown (top to bottom). LBI443 (highlighted by a vertical green shaded bar), is highly conserved across vertebrate species and overlaps five active chromatin-associated marks. (B) *In silico* prediction of transcription factor-binding sites in LBI443 identified five potential binding sites for Lmx1b.

available in the Vista Enhancer Browser, 73 of which have confirmed activity during limb development (Table S5) (Visel et al., 2007). We associated 27 of these PCRMs to 34 genes differentially expressed in the presence of Lmx1b (Table 1). Based on the expression patterns available in the Mouse Genomic Informatics database, we found that the activity of the Lmx1b-bound PCRMs associated with *Osr2*, *Jag1*, *Wnt5a*, *Shox2* and *Cbln4* genes overlapped their respective limb mRNA expression patterns, which also overlaps expression of *Lmx1b* (Loomis et al., 1998; Lan et al., 2001; Witte et al., 2009; Cobb et al., 2006; Haddick et al., 2014).

DISCUSSION

Characteristics of Lmx1b-bound DNA in mouse limbs

We mapped the genome-wide distribution of Lmx1b binding in mouse limbs during limb dorsalization (E12.5). Most of the Lmx1b-bound genomic fragments or intervals (LBIs) mapped to intergenic or intronic regions (Fig. 1A) and associate to active enhancers rather than promoters (Fig. 1D; Fig. S1A,B), a feature shared by other development-related transcription factors (Sheth et al., 2016; McAninch and Thomas, 2014). Based on chromatin regulatory marks (chromatin modifications and bound proteins), nearly 84% (n=617) of the LBIs were categorized as PCRMs.

Development (2017) 144, 2009-2020 doi:10.1242/dev.146332

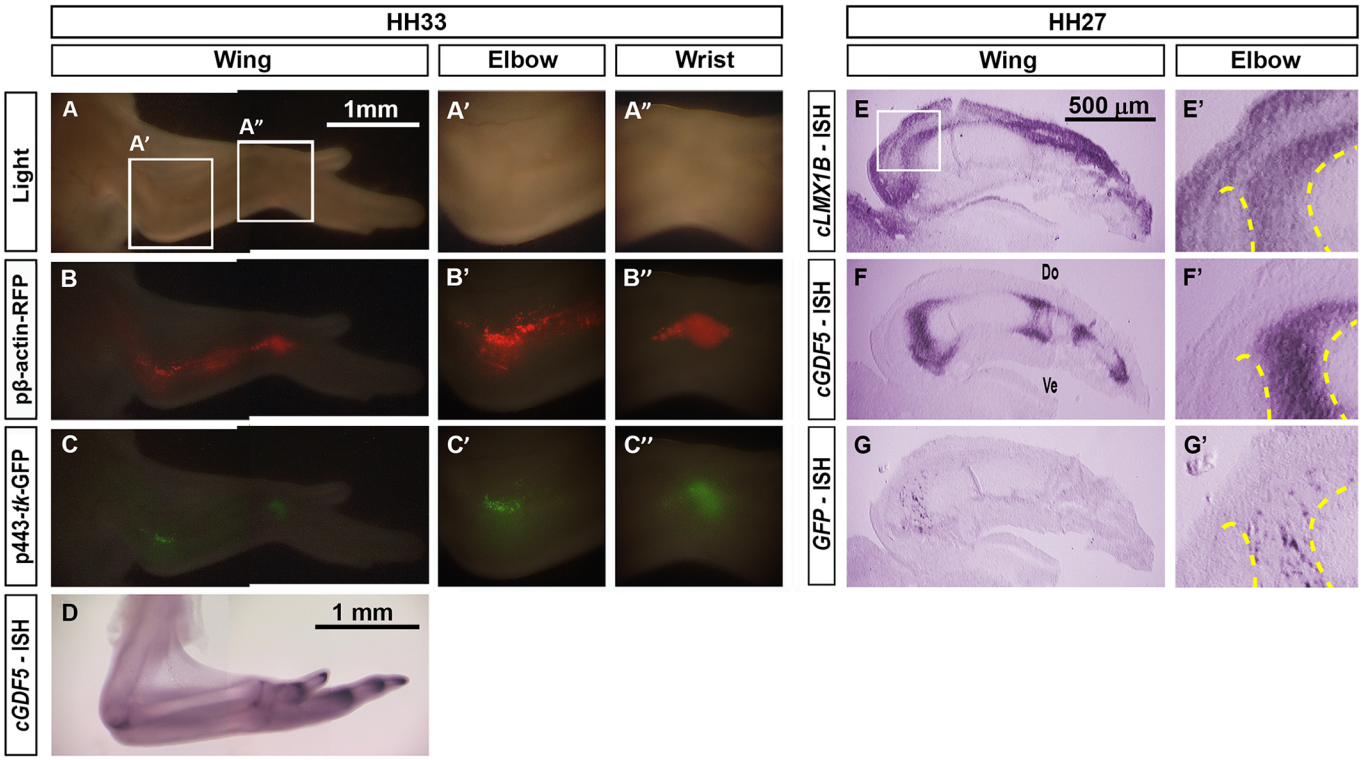

Fig. 6. LBI443 is active in developing *GDF5*-positive joints, with the dorsal aspect extending into the Lmx1b expression domain. (A-C) Composite dorsal view images of HH33 chicken wings 120 h after electroporation (at HH14) showing: (A) morphology with normal light, (B) transfection efficiency using a β-actin promoter-driven RFP plasmid, and (C) functional activity (GFP expression) of the *Gdf5*-associated LBI443 within the elbow and wrist joints. (D) *In situ* hybridization for *GDF5* in HH33 chicken wings (composite dorsal view) shows a pattern of expression within the elbow and wrist that overlaps LBI443 activity. Higher magnification images of the boxed areas are shown in adjacent panels for the elbow (A′-G′) and wrist (A″-C″) regions. Activity was also present in joint digits (data not shown). The fluorescence images (RFP and GFP) of dorsal and transverse views are overlaid with light-field images to denote limb boundaries. (E-G) Section *in situ* hybridization was also performed in HH27 chicken wings 24 h after electroporation to show overlapping *LMX1B* (E,E′), *GDF5* (F,F′) and *GFP* (representing LBI443 activity) expression. Yellow dashed lines in the magnified elbow regions highlight the joint space. Dorsal (Do) and ventral (Ve) aspects are indicated in F.

Typically, the distribution of either repressor (H3k27me3) or active (H3K27ac, RNAP2 or Med12) chromatin regulatory marks is mutually exclusive (Ram et al., 2011; Pasini et al., 2010); remarkably, a small population of Lmx1b-bound PCRMs, such as LBI407, aligned to both active and repressor marks (Fig. 3A; Table S2). This might reflect differences in regulation within the tightly restricted dorsal and ventral compartments of the developing limb, with potentially different genomic landscapes (Arques et al., 2007; Cotney et al., 2013; Andrey et al., 2017) and the capacity for different transcription factors such as Lmx1b to modify activity of these PCRMs. As gene regulation during limb development is a temporally dynamic process, another interpretation could be that the availability or activity of the regulatory sequence is in transition.

Regulatory sequences that are foundational to the development of the vertebrate body plan show high degrees of conservation across species (de Laat and Duboule, 2013). Thus, the conserved PCRMs identified by comparative genomic analysis (n=257) are likely to play crucial roles in Lmx1b-regulated development (Table S2). We validated enhancer activity in two of these conserved PCRMs (LBI407 and LBI443; Figs 4 and 6, respectively) and further confirmed that 80% of the PCRMs that correspond to conserved CRMs have limb activity (Vista Enhancer Browser database; Visel et al., 2007) (Table S5).

Candidate genes for direct Lmx1b regulation

The distance between a regulatory sequence and its target gene can be highly variable and can associate with targets beyond the nearest gene (Marinic et al., 2013; Carter et al., 2002). Genomic territories with enhanced chromatin interactions, called topologically associating domains, can extend over roughly 1 Mb in vertebrates (Dixon et al., 2012). Nearly half of our PCRMs (n=292) were within 1 Mb of an Lmx1b-regulated gene (Fig. 2A; Table S3). The two functionally active PCRMs (LBI407 and LBI443) validated were associated with Lmx1b-regulated genes (*Lmx1b* and *Gdf5*, respectively) with enhancer activity overlapping associated gene expression (Figs 4 and 6). Twenty-seven of the PCRMs confirmed via the Vista Enhancer Browser (Visel et al., 2007) were also linked to Lmx1b-regulated genes (n=34). Five had readily available limb expression patterns that overlapped the associated PCRM/CRM activity (*Osr2*, *Jag1*, *Wnt5a*, *Shox2* and *Cbln4*) (Fig. 7) (Lan et al., 2001; Loomis et al., 1998; McGlinn et al., 2005; Witte et al., 2009; Cobb and Duboule, 2005; Haddick et al., 2014).

PCRMs that were not associated with an Lmx1b-regulated gene at E12.5 are likely to be accessible, but might not be active at this stage. Because limb development is dynamic, stage-specific factors, in addition to Lmx1b binding, might also be required for PCRM activity. Correspondingly, Feenstra and colleagues demonstrated variation in Lmx1b-regulated genes at progressive limb stages (E11.5, E12.5 and E13.5), with less than 10% present across all three stages (Feenstra et al., 2012). Some PCRM-gene associations could also have been missed because of our 1 Mb cut-off for PCRM-target interactions. Although the average CRM-promoter distance is 120 kb (de Laat and Duboule, 2013), interactions have been reported up to a distance of 1.44 Mb (de Laat and Duboule, 2013; Benko et al., 2009).

Development (2017) 144, 2009-2020 doi:10.1242/dev.146332

Table 1. Gene associations to Lmx1b-bound PCRMs with known enhancer activity

LBI	LBI chromosome	LBI start	LBI end	Element	Lmx1b-regulated gene(s)
26	chr1	75833091	75833611	hs1635	*Obsl1*
73	chr10	45230026	45230416	mm87	*Prdm1*
98	chr10	119761840	119762124	hs1498	*Hmga2*
125	chr11	75049646	75050306	hs1445	*Pafah1b1*, *Srr*, *Tlcd2*
133	chr11	87422998	87423326	mm264	*Mir301*
159	chr12	25891661	25892106	hs388	*Id2*
214	chr13	56159816	56160413	hs1473	*Nsd1*
225	chr13	91187223	91188005	hs1432	*Ssbp2*
252	chr14	28972666	28972977	hs1436	*Wnt5a*
285	chr15	35533210	35533643	mm703	*Osr2*
304	chr16	54991738	54992351	hs1469	*Nfkbiz*
333	chr17	47989063	47989453	mm751	*Apobec2*
369	chr18	68909908	68910229	mm708	*Tcf4*
370	chr18	68910647	68911246	mm708	*Tcf4*
398	chr19	60015935	60016244	mm449	*Emx2*, *E330013P04Rik*, *Rab11fip2*
438	chr2	137247962	137248210	hs1278	*Jag1*
439	chr2	137853613	137853963	mm671	*Jag1*
456	chr2	171734144	171735524	hs1448	*Cbln4*
463	chr3	30104643	30105483	hs1433	*Sec62*
464	chr3	30108049	30108319	hs1433	*Sec62*
481	chr3	67070452	67071271	hs741	*Shox2*, *Rsrc1*, *Ptx3*
495	chr3	99665987	99666408	hs1428	*Gm42869*
529	chr4	98223273	98223749	hs1484	*Atg4c*, *Dock7*, *Nfia*
569	chr5	99368833	99369455	mm678	*Prkg2*
582	chr6	4553349	4553603	mm400	*Col1a2*
643	chr7	112826169	112826588	hs1314	*Usp47*
720	chr9	71976098	71976463	hs357	*Gm37879*, *Prtg*, *Tcf12*

List of the 27 Lmx1b-bound potential *cis*-regulatory modules (PCRMs) with functionally validated limb activity (Visel et al., 2007). Genomic coordinates for the Lmx1b-bound intervals and the corresponding element ID of the validated CRM available from the Vista Enhancer Browser (Visel et al., 2007) are shown with the predicted Lmx1b-regulated targets.

Predicted Lmx1b-regulated processes

Gene ontological analysis of candidate PCRM-associated genes predicted target pathways, and tissue systems present in both dorsal and ventral aspects of the limb. Differential compartment-specific regulation of CRMs common to limb tissues is a likely mechanism for refining dorsal asymmetry. Joint development is asymmetric along the dorsal-ventral axis. Growth differentiation factor 5 (*Gdf5*) is a well-established marker for joint development (Settle et al., 2003) with expression spanning both the dorsal and ventral limb compartments. Lmx1b-dependent regulation of the *Gdf5*-associated CRM (LBI443), an enhancer reported to drive *Gdf5* expression in the developing limb joints (Chen et al., 2016), favors a model in which Lmx1b modifies dorsal *Gdf5* enhancer activity.

Lmx1b-dependent regulation of CRMs associated with *Wnt5a* (LBI252) and ECM genes such as keratocan, lumican, decorin and epiphycan (LBI89 and LBI91) (Table S3) are additional mechanisms that could alter limb asymmetry. Wnt5a and ECM components can affect cell growth, survival, differentiation, migration and morphogenesis, which could be regulated differentially along the dorsal-ventral axis (Gros et al., 2010; Rozario and DeSimone, 2010; Koohestani et al., 2013). A role for Lmx1b in ECM regulation has already been demonstrated in the kidney with direct regulation of glomerular basement membrane collagens (Morello et al., 2001).

A role for Lmx1b in axonal guidance was proposed with the identification of targets such as *Cbln4* and *Ntn1* (Krawchuk and Kania, 2008; Feenstra et al., 2012). We demonstrate an Lmx1b-bound CRM (LBI456) associated with *Cbln4* that mimics the pattern of *Cbln4* expression (Visel et al., 2007; Haddick et al., 2014) and two Lmx1b-bound PCRMs (LBI122 and LBI123) that flank *Ntn1* (Table S3), collectively supporting this hypothesis.

Nail-patella syndrome

In humans, haploinsufficiency of *LMX1B* results in nail-patella syndrome (NPS) characterized by nail dysplasia, absent or hypoplastic patellae, bone fragility and premature osteoarthritis (Sweeney et al., 2003). We have identified several Lmx1b-bound PCRMs associated with *Gdf5*, *Sox11* and several ECM-related genes (Tables S3) that are linked to osteoarthritis (Kan et al., 2013; Syddall et al., 2013; Stefansson et al., 2003; Miyamoto et al., 2007).

Another interesting finding suggested by our study is the positive autoregulation of *Lmx1b* expression. In the *Lmx1b* loss-of-function mutant, the *Lmx1b* transcript is reduced 5- to 6-fold (Feenstra et al., 2012). Functional validation of LBI407, located 66 kb upstream of *Lmx1b*, showed dorsally restricted enhancer activity in limb mesoderm coincident with *Lmx1b* expression (Vogel et al., 1995; Riddle et al., 1995; Dreyer et al., 2000). Positive autoregulation provides a mechanism for maintenance or amplification of *Lmx1b* expression following initial activation. Autoregulation during development reinforces or stabilizes a transcriptional pattern of differentiation (Crews and Pearson, 2009). This could also be of clinical importance since a population of NPS patients with mutations linked to the *LMX1B* locus fail to demonstrate mutations in the *LMX1B* coding sequence (Ghoumid et al., 2016). The fact that NPS results from haploinsufficiency of *LMX1B* signifies that the functional level of LMX1B is crucial for normal development. Disruption of the LMX1B autoregulatory system, via mutations in the *LMX1B* CRMs, could therefore account for NPS in families that lack mutations in the coding sequence.

In summary, we have generated a genomic data set of Lmx1b-bound PCRMs during limb dorsalization. Moreover, we have validated and linked Lmx1b-bound *cis*-regulatory modules to genes differentially expressed in the presence of Lxm1b, highlighting the

Development (2017) 144, 2009-2020 doi:10.1242/dev.146332

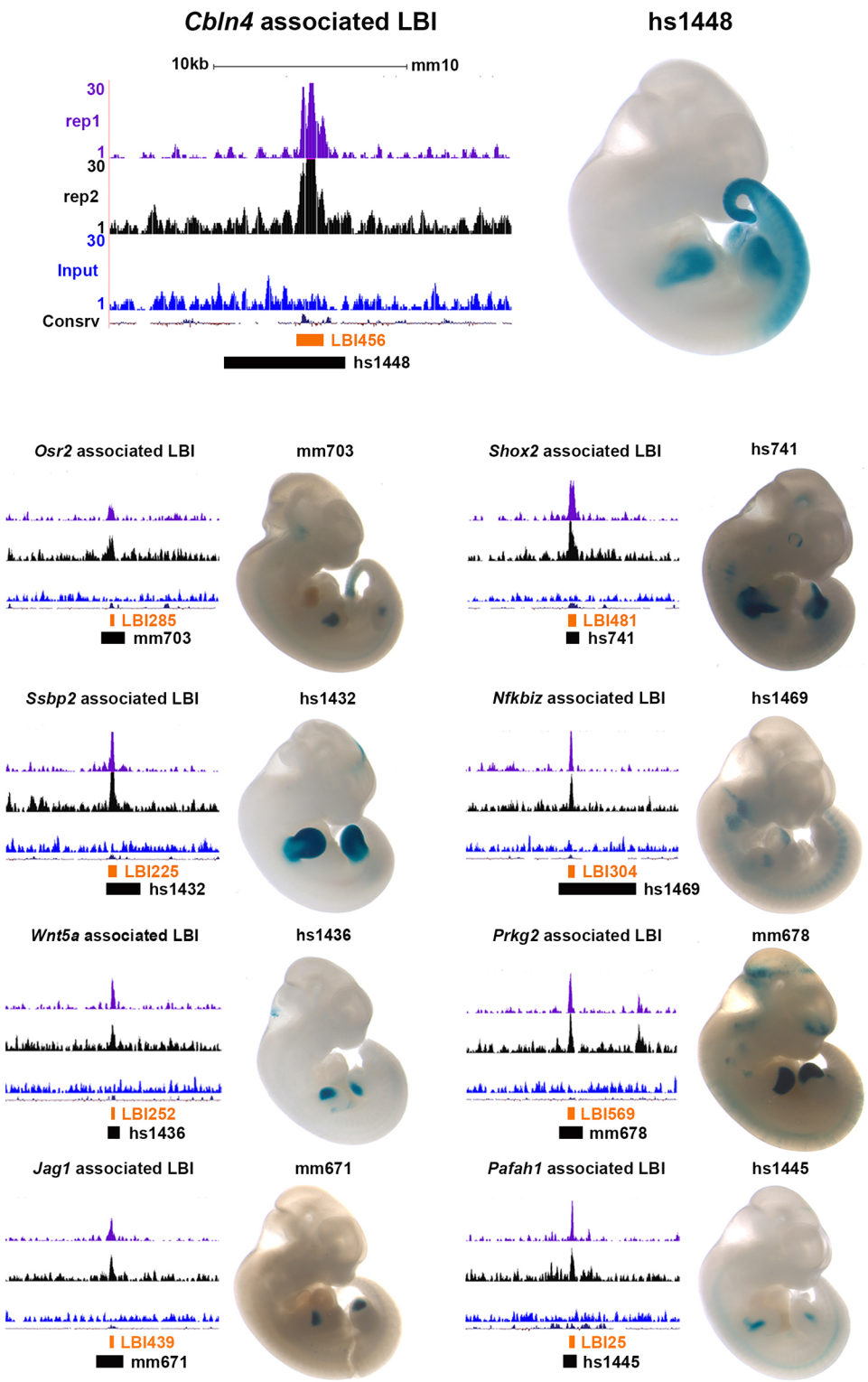

Fig. 7. Lmx1b-bound PCRMs correspond to VISTA Enhancer Browser CRMs. Correlation of nine Lmx1b-bound PCRMs with Vista Enhancer Browser CRMs showing activity in transgenic E11.5 mice. The top panel has the *y*-axis labeled and is enlarged to demonstrate the layout for each interval. The left side of each illustration has a screen shot of the UCSC browser showing –20 kb of genomic DNA with the Lmx1b ChIP-seq tracks (replicate 1, purple; replicate 2, black), input track (blue), the basewise conservation by phylop (Consrv), the Lmx1b-bound interval (LBI, orange) and the corresponding VISTA element (black). On the right of each illustration is a photograph of a transgenic mouse embryo demonstrating the activity of the VISTA element using a *lacZ* (cyan) reporter (used with permission from the Vista Enhancer Browser database; Visel et al., 2007).

processes regulated. These data will allow us to characterize the different mechanisms used by Lmx1b to accomplish limb dorsalization.

MATERIALS AND METHODS

Mouse strains

All animal procedures were performed in accordance with protocols established by the Institutional Animal Care and Use Committee of Loma Linda University. The genetic background of the mouse strain used for this study was C57BL/6. The sex was not determined in the embryos used.

Lmx1b ChIP-seq

Limb tissue from ten E12.5 embryos was pooled for each of the biological replicates (n=2) and submerged in PBS+1% formaldehyde for 15 min. After disruption with a Dounce homogenizer, lysates were sonicated and the DNA sheared to an average length of 300-500 bp. Chromatin (30 µg) was precleared with protein A agarose beads and incubated with 20 µl antibody

Development (2017) 144, 2009-2020 doi:10.1242/dev.146332

against Lmx1b (BMO8) (Suleiman et al., 2007) kindly provided by Dr Witzgall (Institute for Molecular and Cellular Anatomy, University of Regensburg, Germany). The protein-DNA complex was reverse-crosslinked with an overnight incubation in Proteinase K at 65°C. ChIPed DNA was purified by phenol-chloroform extraction and ethanol precipitation.

DNA libraries were quantified and sequenced on Illumina's NextSeq 500. Reads were aligned to the mouse reference genome (mm10) using the default settings for Bowtie algorithm (Li and Durbin, 2009). Lmx1b peak locations were determined using the Model based Analysis for ChIP-seq (MACS) (v1.4.2) (Zhang et al., 2008) with a cutoff of *P*-value=1e-5 (empiric false discovery rate=6-16%).

ChIP validation by qPCR

Chromatin immunoprecipitation for qPCR was performed using ChIP-IT Express Kit (Active Motif) following the manufacturer's recommendations with minor modifications. Lysed cells were sonicated using an Epishear Probe sonicator (Active Motif) to obtain fragments ranging between 300 and 600 bp in length. The sonicated DNA (40 µg), Lmx1b-specific rabbit polyclonal antiserum (20 µl), and 25 µl of protein G beads were incubated overnight at 4°C. DNA elution and de-crosslinking was performed following manufacturer's recommendations. DNA was purified using the QIAquick PCR purification kit (Qiagen).

qPCR (Bio-Rad, CFX96) validation was performed using SYBR-Green (Bio-Rad, 172-5270). Validation was performed in triplicate using two independently generated ChIP samples with the Lmx1b antibody. Primers used for validation of ChIP-qPCR were assayed for primer efficiency and are listed in a 5′ to 3′ orientation in Table S6. Target enrichment was determined by calculating the percentage of target precipitated over the input DNA (% input) and adjusted for primer efficiency. Subsequently, fold enrichment was determined by comparing % input of specific targets over mouse negative control provided in the ChIP-IT qPCR Analysis kit (Active Motif).

Motif discovery

Motif discovery analyses of Lmx1b ChIP-seq-retrieved genomic intervals were performed using the online tool MEME-ChIP 4.11.0 version (http://meme-suite.org/tools/meme-chip) as described by Ma et al. (2014). Input sequences were centered within summit regions of recovered intervals and extended 250 bp in each direction. MEME runs were performed with random subsampling and retrieved motifs between 6 and 10 bp in length with an E-value cut-off of >0.5 for the discovery of enriched motifs.

Genomic regions enrichment of annotations tool

Association of genomic regions to genes was performed using the online tool Genomic Regions Enrichment of Annotations Tool (GREAT; http://bejerano.stanford.edu/great/public-2.0.2/html/) (McLean et al., 2010). Parameters were set so that regulatory domains for genes extended in both directions 1 Mb from the midpoint of the gene's TSS.

Published ChIP-seq data

Limb ChIP-seq data on H3K27ac were obtained at the National Center for Biotechnology Information (NCBI) from the Gene Expression Omnibus database (GEO; http://www.ncbi.nlm.nih.gov/geo/) under accession numbers GSE30641 and GSE42413, p300 under accession number GSE13845, and both H3K27me3 and H3K4me2 under the accession number GSE42237. RNAP2 and Med12 ChIP-seq data were obtained from Berlivet et al. (Berlivet et al., 2013). The data for comparison were converted to the mouse build mm10 using the UCSC liftover tool. Lmx1b ChIP-seq-retrieved genomic intervals were extended 250 bp in both directions for comparison with published ChIP-seq data.

Comparative analyses

Comparative analysis of Lmx1b ChIP-seq-identified intervals was performed by pairwise alignment (Vista browser; http://genome.lbl.gov/vista/). Species selected for the pairwise alignment comparison were mouse, human, horse and chicken. An interval was considered conserved when it exhibited at least a 70% homology.

Gene ontology

Lmx1b-regulated genes associated with LBIs were classified according to Gene Ontology terms using Ingenuity Pathway Analysis (IPA) software and database (Qiagen).

Isolation and cloning of potential regulatory regions

The two LBIs analyzed were isolated from mouse genomic DNA by PCR using the following primer pairs:

LBI407 (1226 bp fragment), 5′-GGGGACCAGGAGAAATATTACA GTGTG-3′ and 5′-CAGAATCCCCCCAGAGATAGATGC-3′; LBI443 (867 bp fragment), 5′-CTACAGCTCAGTCTCCTTCAGGCTACAC-3′ and 5′-CCATACATACTGAGCCACCACATGG-3′.

The PCR products were cloned into pCR-II TOPO vector (Qiagen) for subsequent subcloning into a thymidine kinase (*tk*) promoter-driven GFP reporter construct for functional analyses (Uchikawa et al., 2003).

Functional enhancer assays

Minimal promoter-driven GFP reporter constructs bearing the potential regulatory region of interest were delivered into presumptive limb region of Hamburger and Hamilton stage (HH) 14 chicken embryos as previously described by Pira and colleagues (Pira et al., 2008). Transfection efficiency was assessed by co-electroporation of a β-actin promoter-driven RFP construct. Electroporation was performed using the CUY21 electroporation station (Protech International). Depending on the construct of interest, embryos were incubated for 2-5 days before harvesting for visualization of GFP activity and digital image acquisition (Sony DKC-5000).

In situ hybridization and probe generation

Whole-mount *in situ* hybridization was performed as described by Yamada et al. (1999). Section *in situ* hybridization was performed as described (Moorman et al., 2001). *GDF5* and *LMX1B* probes were generated by RT-PCR as described by Merino et al. (1998) using the following primer pairs: cGDF5, 5′-GTAAGGACGGTGACTCCAAAGG-3′ and 5′-CCTT GCCTTCAGGTTCTTACTG-3′; cLMX1B, 5′-GGATCGCTTTCTGAT GAGG-3′ and 5′-GATGTCATCATTCCTTCCATTCG-3′.

Acknowledgements

The authors would like to thank Dr Ralph Witzgall for the kind gift of the Lmx1b antibody (BMO8); Drs Nadav Ahituv, Thomas Girke and Paul Labhart for assistance and suggestions regarding data analysis and standardization; and Drs Salva Soriano and Brendon Gongol for critical review of the manuscript.

Competing interests

The authors declare no competing or financial interests.

Author contributions

Conceptualization: E.H., J.M.F., K.C.O.; Methodology: E.H., J.M.F., C.U.P., S.M., K.C.O.; Software: E.H., K.C.O.; Validation: E.H., B.A.W., J.M.F., L.T.; Formal analysis: E.H., B.A.W., L.T., K.C.O.; Investigation: E.H., L.T., C.U.P.; Data curation: E.H., B.A.W.; Writing - original draft: E.H., K.C.O.; Writing - review & editing: E.H., B.A.W., J.M.F., L.T., C.U.P., S.M., K.C.O.; Visualization: E.H., B.A.W., L.T., C.U.P., K.C.O.; Supervision: C.U.P., S.M., K.C.O.; Project administration: K.C.O.; Funding acquisition: K.C.O.

Funding

This work was supported in part by grants from the National Organization for Rare Disorders (K.C.O.) and the Loma Linda University Pathology Research Endowment Fund (K.C.O.).

Data availability

The Lmx1b-ChIP-seq data sets reported in the paper are available through Gene Expression Omnibus under accession number GSE84064 (https://www.ncbi.nlm.nih.gov/geo/query/acc.cgi?acc=GSE84064).

Supplementary information

Supplementary information available online at
http://dev.biologists.org/lookup/doi/10.1242/dev.146332.supplemental

References

Andrey, G., Schöpflin, R., Jerković, I., Heinrich, V., Ibrahim, D. M., Paliou, C., Hochradel, M., Timmermann, B., Haas, S., Vingron, M. et al. (2017).

Development (2017) 144, 2009-2020 doi:10.1242/dev.146332

Characterization of hundreds of regulatory landscapes in developing limbs reveals two regimes of chromatin folding. *Genome Res.* **27**, 223-233.

Arques, C. G., Doohan, R., Sharpe, J. and Torres, M. (2007). Cell tracing reveals a dorsoventral lineage restriction plane in the mouse limb bud mesenchyme. *Development* **134**, 3713-3722.

Asbreuk, C. H., Vogelaar, C. F., Hellemons, A., Smidt, M. P. and Burbach, J. P. (2002). CNS expression pattern of Lmx1b and coexpression with ptx genes suggest functional cooperativity in the development of forebrain motor control systems. *Mol Cell Neurosci.* **21**, 410-420.

Bailey, T. L., Johnson, J., Grant, C. E. and Noble, W. S. (2015). The MEME suite. *Nucleic Acids Res.* **43**, W39-W49.

Bell, S. M., Schreiner, C. M. and Scott, W. J. (1998). The loss of ventral ectoderm identity correlates with the inability to form an AER in the legless hindlimb bud. *Mech. Dev.* **74**, 41-50.

Benko, S., Fantes, J. A., Amiel, J., Kleinjan, D.-J., Thomas, S., Ramsay, J., Jamshidi, N., Essafi, A., Heaney, S., Gordon, C. T. et al. (2009). Highly conserved non-coding elements on either side of SOX9 associated with Pierre Robin sequence. *Nat. Genet.* **41**, 359-364.

Berlivet, S., Paquette, D., Dumouchel, A., Langlais, D., Dostie, J. and Kmita, M. (2013). Clustering of tissue-specific sub-TADs accompanies the regulation of HoxA genes in developing limbs. *PLoS Genet.* **9**, e1004018.

Carter, D., Chakalova, L., Osborne, C. S., Dai, Y. F. and Fraser, P. (2002). Long-range chromatin regulatory interactions in vivo. *Nat. Genet.* **32**, 623-626.

Chen, H., Lun, Y., Ovchinnikov, D., Kokubo, H., Oberg, K. C., Pepicelli, C. V., Gan, L., Lee, B. and Johnson, R. L. (1998). Limb and kidney defects in Lmx1b mutant mice suggest an involvement of LMX1B in human nail patella syndrome. *Nat. Genet.* **19**, 51-55.

Chen, H., Capellini, T. D., Schoor, M., Mortlock, D. P., Reddi, A. H. and Kingsley, D. M. (2016). Heads, shoulders, elbows, knees, and toes: modular Gdf5 enhancers control different joints in the vertebrate skeleton. *PLoS Genet.* **12**, e1006454.

Cobb, J. and Duboule, D. (2005). Comparative analysis of genes downstream of the Hoxd cluster in developing digits and external genitalia. *Development* **132**, 3055-3067.

Cobb, J., Dierich, A., Huss-Garcia, Y. and Duboule, D. (2006). A mouse model for human short-stature syndromes identifies Shox2 as an upstream regulator of Runx2 during long-bone development. *Proc. Natl. Acad. Sci. USA* **103**, 4511-4515.

Cotney, J., Leng, J., Yin, J., Reilly, S. K., Demare, L. E., Emera, D., Ayoub, A. E., Rakic, P. and Noonan, J. P. (2013). The evolution of lineage-specific regulatory activities in the human embryonic limb. *Cell* **154**, 185-196.

Crews, S. T. and Pearson, J. C. (2009). Transcriptional autoregulation in development. *Curr. Biol.* **19**, R241-R246.

Cygan, J. A., Johnson, R. L. and Mcmahon, A. P. (1997). Novel regulatory interactions revealed by studies of murine limb pattern in Wnt-7a and En-1 mutants. *Development* **124**, 5021-5032.

De Laat, W. and Duboule, D. (2013). Topology of mammalian developmental enhancers and their regulatory landscapes. *Nature* **502**, 499-506.

Demare, L. E., Leng, J., Cotney, J., Reilly, S. K., Yin, J., Sarro, R. and Noonan, J. P. (2013). The genomic landscape of cohesin-associated chromatin interactions. *Genome Res.* **23**, 1224-1234.

Dixon, J. R., Selvaraj, S., Yue, F., Kim, A., Li, Y., Shen, Y., Hu, M., Liu, J. S. and Ren, B. (2012). Topological domains in mammalian genomes identified by analysis of chromatin interactions. *Nature* **485**, 376-380.

Dreyer, S. D., Morello, R., German, M. S., Zabel, B., Winterpacht, A., Lunstrum, G. P., Horton, W. A., Oberg, K. C. and Lee, B. (2000). LMX1B transactivation and expression in nail-patella syndrome. *Hum. Mol. Genet.* **9**, 1067-1074.

Feenstra, J. M., Kanaya, K., Pira, C. U., Hoffman, S. E., Eppey, R. J. and Oberg, K. C. (2012). Detection of genes regulated by Lmx1b during limb dorsalization. *Dev. Growth Differ.* **54**, 451-462.

Frazer, K. A., Pachter, L., Poliakov, A., Rubin, E. M. and Dubchak, I. (2004). VISTA: computational tools for comparative genomics. *Nucleic Acids Res.* **32**, W273-W279.

Ghoumid, J., Petit, F., Holder-Espinasse, M., Jourdain, A.-S., Guerra, J., Dieux-Coeslier, A., Figeac, M., Porchet, N., Manouvrier-Hanu, S. and Escande, F. (2016). Nail-Patella Syndrome: clinical and molecular data in 55 families raising the hypothesis of a genetic heterogeneity. *Eur. J. Hum. Genet.* **24**, 44-50.

Gros, J., Hu, J. K.-H., Vinegoni, C., Feruglio, P. F., Weissleder, R. and Tabin, C. J. (2010). WNT5A/JNK and FGF/MAPK pathways regulate the cellular events shaping the vertebrate limb bud. *Curr. Biol.* **20**, 1993-2002.

Gu, W. X. W. and Kania, A. (2010). Identification of genes controlled by LMX1B in E13.5 mouse limbs. *Dev. Dyn.* **239**, 2246-2255.

Haddick, P. C. G., Tom, I., Luis, E., Quiñones, G., Wranik, B. J., Ramani, S. R., Stephan, J.-P., Tessier-Lavigne, M. and Gonzalez, L. C. (2014). Defining the ligand specificity of the deleted in colorectal cancer (DCC) receptor. *PLoS ONE.* **9**, e84823.

Hardison, R. C. and Taylor, J. (2012). Genomic approaches towards finding cis-regulatory modules in animals. *Nat. Rev. Genet.* **13**, 469-483.

Heintzman, N. D., Hon, G. C., Hawkins, R. D., Kheradpour, P., Stark, A., Harp, L. F., Ye, Z., Lee, L. K., Stuart, R. K., Ching, C. W. et al. (2009). Histone modifications at human enhancers reflect global cell-type-specific gene expression. *Nature* **459**, 108-112.

Kagey, M. H., Newman, J. J., Bilodeau, S., Zhan, Y., Orlando, D. A., Van Berkum, N. L., Ebmeier, C. C., Goossens, J., Rahl, P. B., Levine, S. S. et al. (2010). Mediator and cohesin connect gene expression and chromatin architecture. *Nature* **467**, 430-435.

Kan, A., Ikeda, T., Fukai, A., Nakagawa, T., Nakamura, K., Chung, U. I., Kawaguchi, H. and Tabin, C. J. (2013). SOX11 contributes to the regulation of GDF5 in joint maintenance. *BMC Dev. Biol.* **13**, 4.

Koohestani, F., Braundmeier, A. G., Mahdian, A., Seo, J., Bi, J. J. and Nowak, R. A. (2013). Extracellular matrix collagen alters cell proliferation and cell cycle progression of human uterine leiomyoma smooth muscle cells. *PLoS ONE* **8**, e75844.

Krawchuk, D. and Kania, A. (2008). Identification of genes controlled by LMX1B in the developing mouse limb bud. *Dev. Dyn.* **237**, 1183-1192.

Lan, Y., Kingsley, P. D., Cho, E.-S. and Jiang, R. (2001). Osr2, a new mouse gene related to Drosophila odd-skipped, exhibits dynamic expression patterns during craniofacial, limb, and kidney development. *Mech. Dev.* **107**, 175-179.

Li, H. and Durbin, R. (2009). Fast and accurate short read alignment with Burrows-Wheeler transform. *Bioinformatics* **25**, 1754-1760.

Loomis, C. A., Harris, E., Michaud, J., Wurst, W., Hanks, M. and Joyner, A. L. (1996). The mouse Engrailed-1 gene and ventral limb patterning. *Nature* **382**, 360-363.

Loomis, C. A., Kimmel, R. A., Tong, C. X., Michaud, J. and Joyner, A. L. (1998). Analysis of the genetic pathway leading to formation of ectopic apical ectodermal ridges in mouse Engrailed-1 mutant limbs. *Development* **125**, 1137-1148.

Ma, W., Noble, W. S. and Bailey, T. L. (2014). Motif-based analysis of large nucleotide data sets using MEME-ChIP. *Nat. Protoc.* **9**, 1428-1450.

Marinić, M., Aktas, T., Ruf, S. and Spitz, F. (2013). An integrated holo-enhancer unit defines tissue and gene specificity of the Fgf8 regulatory landscape. *Dev. Cell* **24**, 530-542.

Mcaninch, D. and Thomas, P. (2014). Identification of highly conserved putative developmental enhancers bound by SOX3 in neural progenitors using ChIP-Seq. *PLoS ONE* **9**, e113361.

McGlinn, E., Van Bueren, K. L., Fiorenza, S., Mo, R., Poh, A. M., Forrest, A., Soares, M. B., Bonaldo Mde., F., Grimmond, S., Hui, C. C. et al. (2005). Pax9 and Jagged1 act downstream of Gli3 in vertebrate limb development. *Mech. Dev.* **122**, 1218-1233.

Mclean, C. Y., Bristor, D., Hiller, M., Clarke, S. L., Schaar, B. T., Lowe, C. B., Wenger, A. M. and Bejerano, G. (2010). GREAT improves functional interpretation of cis-regulatory regions. *Nat. Biotechnol.* **28**, 495-501.

Merino, R., Gañan, Y., Macias, D., Economides, A. N., Sampath, K. T. and Hurle, J. M. (1998). Morphogenesis of digits in the avian limb is controlled by FGFs, TGFbetas, and noggin through BMP signaling. *Dev. Biol.* **200**, 35-45.

Miyamoto, Y., Mabuchi, A., Shi, D., Kubo, T., Takatori, Y., Saito, S., Fujioka, M., Sudo, A., Uchida, A., Yamamoto, S. et al. (2007). A functional polymorphism in the 5′ UTR of GDF5 is associated with susceptibility to osteoarthritis. *Nat. Genet.* **39**, 529-533.

Moorman, A. F. M., Houweling, A. C., de Boer, P. A. J. and Christoffels, V. M. (2001). Sensitive nonradioactive detection of mRNA in tissue sections: novel application of the whole-mount in situ hybridization protocol. *J. Histochem. Cytochem.* **49**, 1-8.

Morello, R., Zhou, G., Dreyer, S. D., Harvey, S. J., Ninomiya, Y., Thorner, P. S., Miner, J. H., Cole, W., Winterpacht, A., Zabel, B. et al. (2001). Regulation of glomerular basement membrane collagen expression by LMX1B contributes to renal disease in nail patella syndrome. *Nat. Genet.* **27**, 205-208.

Parr, B. A. and Mcmahon, A. P. (1995). Dorsalizing signal Wnt-7a required for normal polarity of D-V and A-P axes of mouse limb. *Nature* **374**, 350-353.

Pasini, D., Malatesta, M., Jung, H. R., Walfridsson, J., Willer, A., Olsson, L., Skotte, J., Wutz, A., Porse, B., Jensen, O. N. et al. (2010). Characterization of an antagonistic switch between histone H3 lysine 27 methylation and acetylation in the transcriptional regulation of Polycomb group target genes. *Nucleic Acids Res.* **38**, 4958-4969.

Pira, C. U., Caltharp, S. A., Kanaya, K., Manu, S. K., Greer, L. F. and Oberg, K. C. (2008). Identification of developmental enhancers using targeted regional electroporation (TREP) of evolutionarily conserved regions. In *Bioluminescence and Chemiluminescence. Light Emission: Biology and Scientific Applications* (ed. X. Shen, X.-L. Yang, X.-R. Zhang, Z. L. Cui, L. J. Kricka and P. E. Stanley), p. 319-322. Singapore: World Scientific Publishing.

Pizette, S., Abate-Shen, C. and Niswander, L. (2001). BMP controls proximodistal outgrowth, via induction of the apical ectodermal ridge, and dorsoventral patterning in the vertebrate limb. *Development* **128**, 4463-4474.

Ram, O., Goren, A., Amit, I., Shoresh, N., Yosef, N., Ernst, J., Kellis, M., Gymrek, M., Issner, R., Coyne, M. et al. (2011). Combinatorial patterning of chromatin regulators uncovered by genome-wide location analysis in human cells. *Cell* **147**, 1628-1639.

Riddle, R. D., Ensini, M., Nelson, C., Tsuchida, T., Jessell, T. M. and Tabin, C. (1995). Induction of the LIM homeobox gene Lmx1 by WNT7a establishes dorsoventral pattern in the vertebrate limb. *Cell* **83**, 631-640.

Development (2017) 144, 2009-2020 doi:10.1242/dev.146332

Rozario, T. and Desimone, D. W. (2010). The extracellular matrix in development and morphogenesis: a dynamic view. *Dev. Biol.* **341**, 126-140.

Settle, S. H., Jr, Rountree, R. B., Sinha, A., Thacker, A., Higgins, K. and Kingsley, D. M. (2003). Multiple joint and skeletal patterning defects caused by single and double mutations in the mouse Gdf6 and Gdf5 genes. *Dev. Biol.* **254**, 116-130.

Sheth, R., Barozzi, I., Langlais, D., Osterwalder, M., Nemec, S., Carlson, H. L., Stadler, H. S., Visel, A., Drouin, J. and Kmita, M. (2016). Distal Limb Patterning Requires Modulation of cis-Regulatory Activities by HOX13. *Cell Rep.* **17**, 2913-2926.

Stefánsson, S. E., Jónsson, H., Ingvarsson, T., Manolescu, I., Jónsson, H. H., Ólafsdóttir, G., Pálsdóttir, E., Stefánsdóttir, G., Sveinbjörnsdóttir, G., Frigge, M. L. et al. (2003). Genomewide scan for hand osteoarthritis: a novel mutation in matrilin-3. *Am. J. Hum. Genet.* **72**, 1448-1459.

Suleiman, H., Heudobler, D., Raschta, A.-S., Zhao, Y., Zhao, Q., Hertting, I., Vitzthum, H., Moeller, M. J., Holzman, L. B., Rachel, R. et al. (2007). The podocyte-specific inactivation of Lmx1b, Ldb1 and E2a yields new insight into a transcriptional network in podocytes. *Dev. Biol.* **304**, 701-712.

Sweeney, E., Fryer, A., Mountford, R., Green, A. and Mcintosh, I. (2003). Nail patella syndrome: a review of the phenotype aided by developmental biology. *J. Med. Genet.* **40**, 153-162.

Syddall, C. M., Reynard, L. N., Young, D. A. and Loughlin, J. (2013). The identification of trans-acting factors that regulate the expression of GDF5 via the osteoarthritis susceptibility SNP rs143383. *PLoS Genet.* **9**, e1003557.

Towers, A. L., Clay, C. A., Sereika, S. M., Mcintosh, I. and Greenspan, S. L. (2005). Skeletal integrity in patients with nail patella syndrome. *J. Clin. Endocrinol. Metab.* **90**, 1961-1965.

Uchikawa, M., Ishida, Y., Takemoto, T., Kamachi, Y. and Kondoh, H. (2003). Functional analysis of chicken Sox2 enhancers highlights an array of diverse regulatory elements that are conserved in mammals. *Dev. Cell.* **4**, 509-519.

Visel, A., Minovitsky, S., Dubchak, I. and Pennacchio, L. A. (2007). VISTA enhancer browser–a database of tissue-specific human enhancers. *Nucleic Acids Res.* **35**, D88-D92.

Visel, A., Blow, M. J., Li, Z., Zhang, T., Akiyama, J. A., Holt, A., Plajzer-Frick, I., Shoukry, M., Wright, C., Chen, F. et al. (2009). ChIP-seq accurately predicts tissue-specific activity of enhancers. *Nature* **457**, 854-858.

Vogel, A., Rodriguez, C., Warnken, W. and Belmonte, J. C. I. (1995). Dorsal cell fate specified by chick Lmx1 during vertebrate limb development. *Nature* **378**, 716-720.

Witte, F., Dokas, J., Neuendorf, F., Mundlos, S. and Stricker, S. (2009). Comprehensive expression analysis of all Wnt genes and their major secreted antagonists during mouse limb development and cartilage differentiation. *Gene Expr. Patterns* **9**, 215-223.

Yamada, M., Szendro, P. I., Prokscha, A., Schwartz, R. J. and Eichele, G. (1999). Evidence for a role of Smad6 in chick cardiac development. *Dev. Biol.* **215**, 48-61.

Zhang, Y., Liu, T., Meyer, C. A., Eeckhoute, J., Johnson, D. S., Bernstein, B. E., Nusbaum, C., Myers, R. M., Brown, M., Li, W. et al. (2008). Model-based analysis of ChIP-Seq (MACS). *Genome Biol.* **9**, R137.

Supplemental Information

Table S1. Lmx1b-ChIP-seq intervals in E12.5 mouse limb.

Tabulated format of the genomic intervals bound by Lmx1b (LBI) that were identified in mouse limbs (E12.5) in both ChIP-seq replicates. Corresponding chromosome (chr), genomic location in mouse (mm10 reference genome) (LBI-Start and LBI-end), interval length, peak summit, peak value, average value (Avg Val) and bin count are listed (1).

Click here to Download Table S1

Table S2. Correlation between Lmx1b-bound Intervals and Chromatin Regulatory Marks.

Comparative analysis of Lmx1b-bound (LBI) intervals to p300, H3K27Ac, H3K4me2, RNA Pol II, Med12, and H3K27me3 ChIP-seq data. Conservation of each Lmx1b-bound interval is also indicated. The data is sorted by the number of chromatin regulatory marks (# of Marks) and by whether both active and repressor marks were present (Both marks). The shaded columns were not used to determine the number of regulatory marks. A potential regulatory modules (PCRM) is an Active-PCRM if has at least two chromatin regulatory marks associated.

Click here to Download Table S2

Table S3. Target genes of Lmx1b-bound potential regulatory regions

Comparison of Lmx1b-bound potential regulatory modules (PCRMs) and genes differentially expressed in the presence of Lmx1b. A total of 292 PCRMs are associated to 254 genes (Assoc gene). Note that there are multiple PCRMs associated to different genes and several genes are associated to multiple PCRMs. LBI corresponds to Lmx1b-bound interval number from table S1 for reference. The PCRMs are categorized base on their chromatin regulatory marks (Reg Marks).. If both active and repressor chromatin regulatory marks are present the PCRM is classified as Both-PCRM (See S2 for reference). The background color in this column indicates whether the associated genes are upregulated (red) downregulated (green) or whether the PCRM has both upregulated and downregulated (yellow) gene associations. The distance from the gene to the PCRM (Distance) is included with the fold change (Fold) and p-values from the published gene array data (Feenstra et al., 2012).

Click here to Download Table S3

Table S4. Lmx1b-PCRM-associated genes present within functional categories

PCRM associated genes classified according to functional categories and annotated functions as outlined in Figure 2C & D. P-value, number and names of molecules in each assigned category are specified if available**.**

Click here to Download Table S4

Table S5. Lmx1b bound Potential Cis Regulatory Modules (PCRMs) that correspond to functionally validated elements from the VISTA enhancer browser.

List of 91 Lmx1b bound PCRMs and corresponding element ID of the VISTA elements - (Visel et al., 2007), followed by the candidate target gene ID and enhancer activity of the tested element. Note that 71 Lmx1b bound PCRMs are functionally active according to the VISTA elements available form the VISTA enhancer browser.

Click here to Download Table S5

Table S6. Primers used for ChIP-qPCR Validation

Lmx1b bound Interval (LBI) number and primers sequence for the specified potential target validation by ChIP-qPCR. Primers are in a 5' to 3' orientation.

Click here to Download Table S6

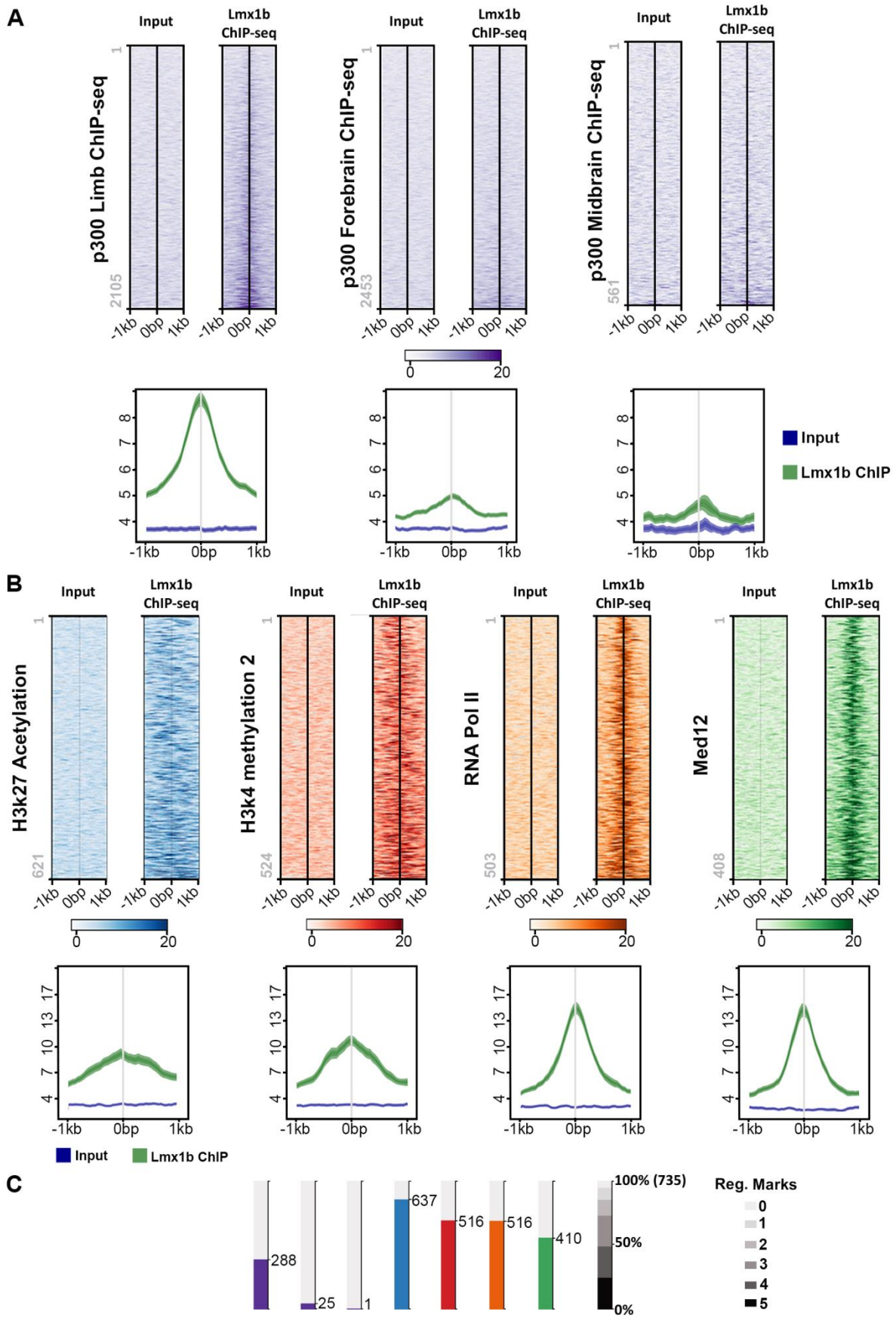

Figure S1. Lmx1b bound intervals display a distribution that corresponded to a limb specific pattern and are enriched in genomic regions associated to active regulation.

A) Heatmap (top) and summarized average plots (bottom) showing the distribution of tagged sequences retrieved from the Lmx1b ChIP-seq and input DNA from limb tissue around p300 ChIP-seq intervals in limb, forebrain and midbrain (Visel et al., 2009). More Lmx1b tagged sequences overlap with p300 intervals in the limb than in the forebrain or midbrain with a 3-fold enrichment for the Lmx1b ChIP-seq retrieved tagged sequences over input DNA. B) Distribution of Lmx1b ChIP-seq and input retrieved tagged sequences around regions associated to active regulation determined by ChIP-seq (H3k27Ac, H3Kme2, RNA Pol II and Med12) (Visel et al., 2009, Berlivet et al., 2013, Cotney et al., 2013, DeMare et al., 2013) that overlapped Lmx1b bound intervals (LBI). Lmx1b ChIP-seq tagged sequences are enriched (~3-fold) within genomic regions associated to chromatin regulatory marks (H3K27Ac, H3K4me2) in comparison to input DNA and it is greater (4-fold) around regulatory regions undergoing active transcription (RNA Pol II, Med12). C) Bar graph depicting the number of LBIs that overlap with the different marks associated to cis-regulatory activity, where the number the percentage of LBIs overlapping chromatin regulatory marks. Note that the colors for each of the marks matched those used above for the heatmaps.

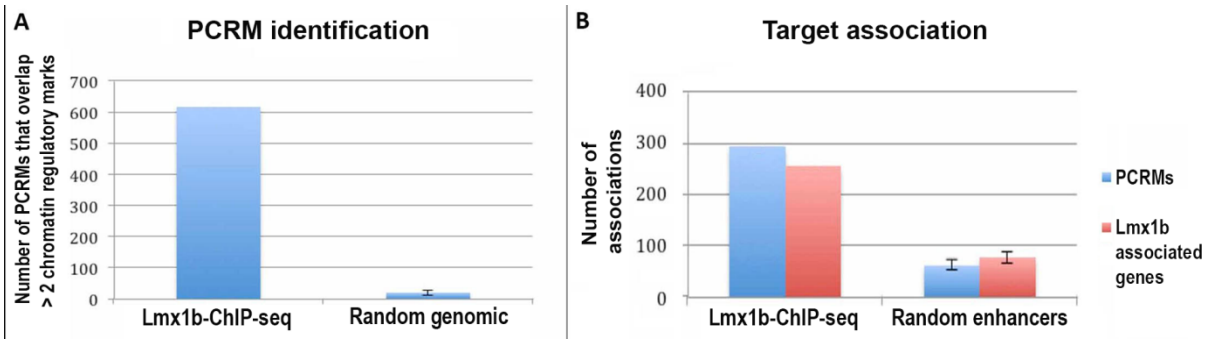

Figure S2. Enrichment of marks associated to potential cis-regulatory modules and Lmx1b regulated genes in Lmx1b bound intervals potential cis regulatory modules.

A) Overlap with at least 2 chromatin regulatory marks yields a 30 times higher number of potential cis-regulatory modules (PCRM) identified in the Lmx1b ChIP-seq dataset (617) in comparison to randomly selected genomic regions (n=5 groups, each with 735 random genomic intervals, One sample t-test p<1e-4, mean19.6 ±6.6). B) Lmx1b bound PCRMs are enriched within Lmx1b regulated genes. The number of PCRM associated to Lmx1b regulated genes is ~5 times higher within Lmx1b identified PCRMs (292) compared to randomly selected enhancer regions based on H3K27Ac (Cotney et al., 2013) (n=5 groups, each with 292 random genomic intervals, One sample t-test p<1e-4, mean 60.6 ±7.1) and ~3 times higher for the number of Lmx1b regulated genes associated to a PCRM (n=5 groups, each with 292 random genomic intervals, One sample t-test p<1e-4, mean 75.8 ±10.8).

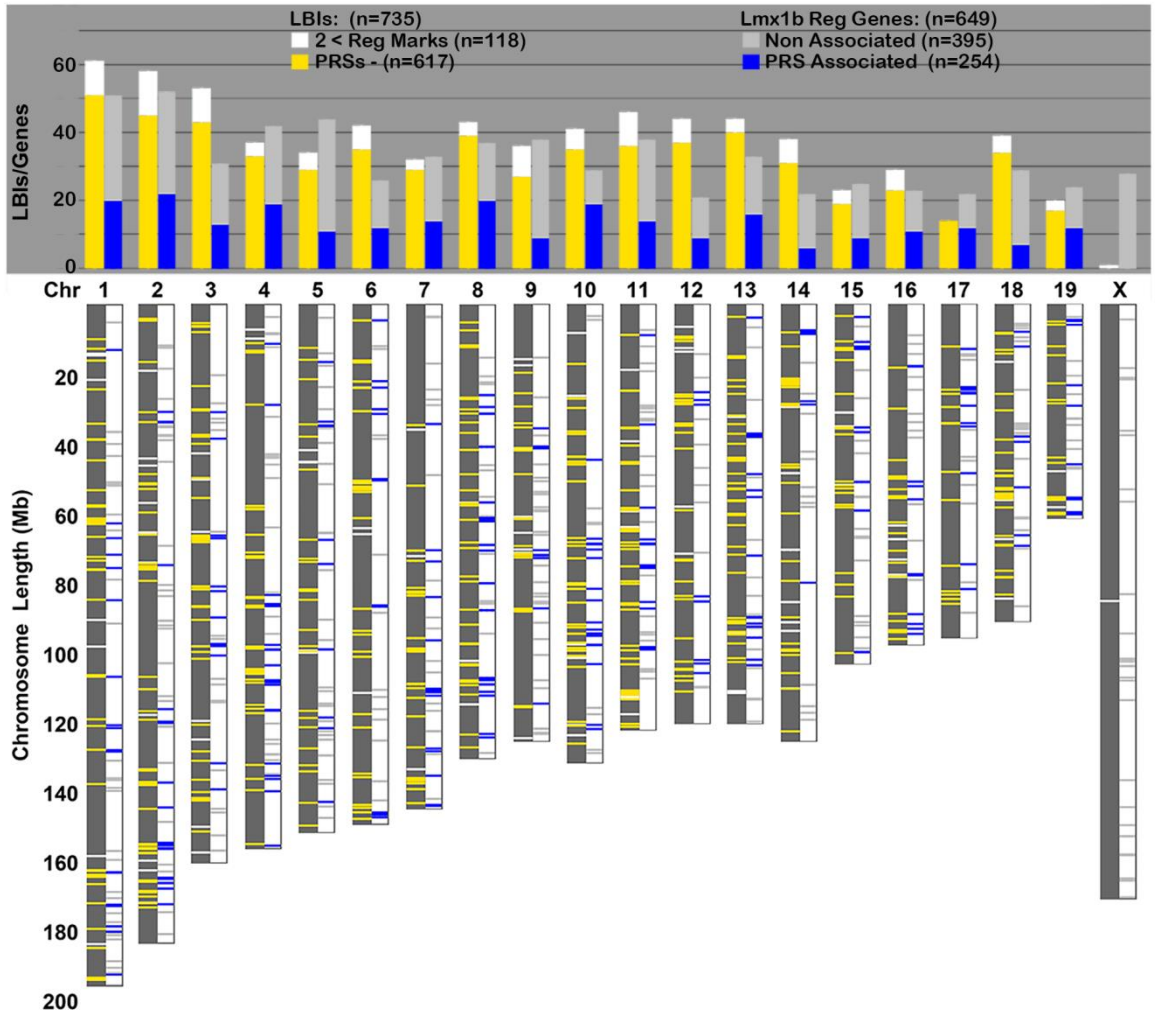

Figure S3. Distribution of Lmx1b-bound PCRMs and associated Lmx1b-regulated genes

The genomic distribution of Lmx1b bound intervals (LBIs) is represented on mouse chromosomes. Yellow marks along the chromosome indicate potential *cis*-regulatory modules (PCRMs), while light grey marks indicate LBIs that do not meet our criterion of a PCRM (≥ 2 chromatin regulatory marks). Location of Lmx1b-regulated genes at E12.5

(Feenstra et al., 2012) are indicated beside each chromosome, blue indicates association with a PCRM and dark grey indicates non-associated genes. A summary of the PCRM and gene distribution is shown above the chromosomes. No Lmx1b-bound PCRMs are identified within the X chromosome.

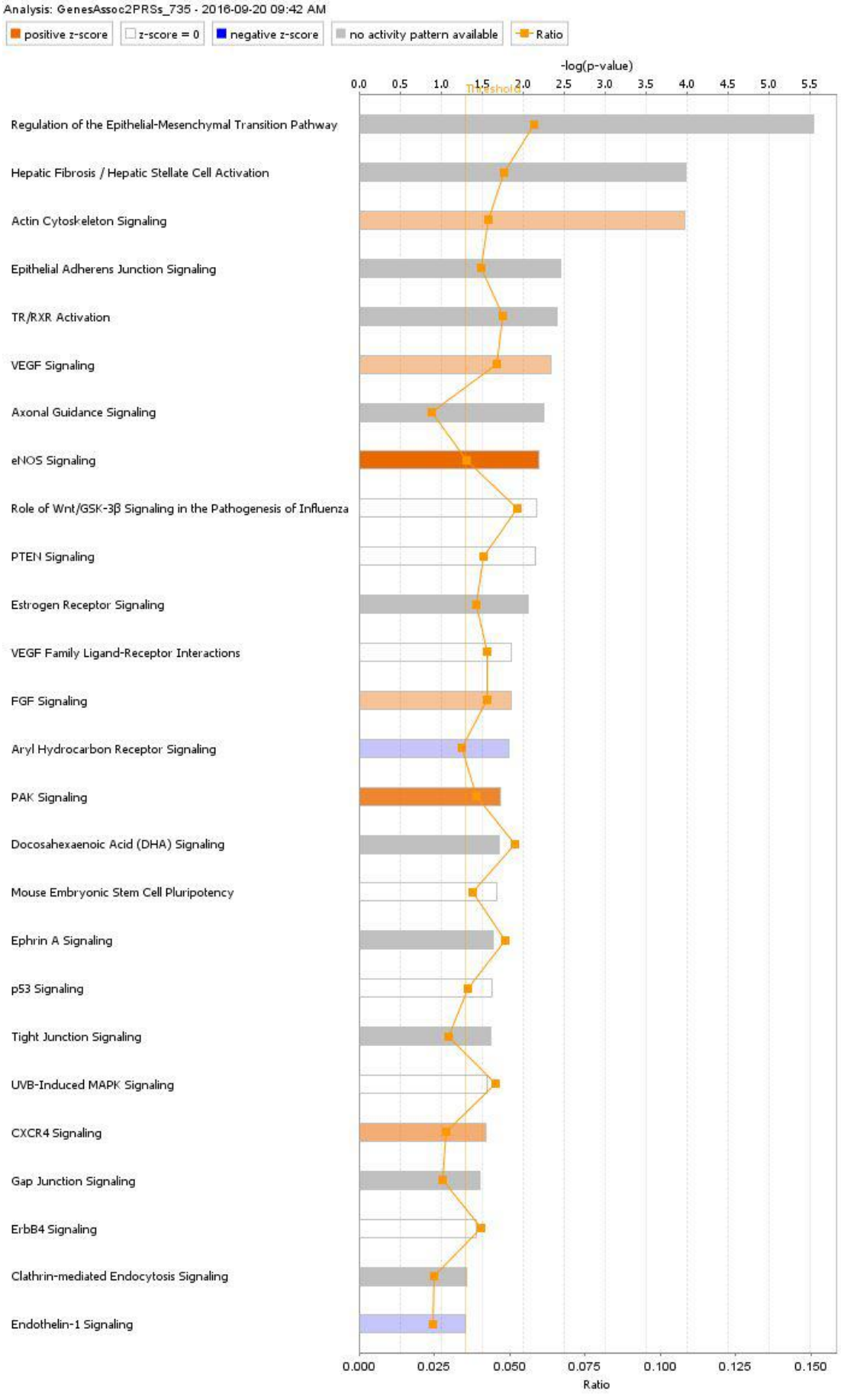

Figure S4. Prediction of canonical pathways affected

Bar-chart representation of pathways affected according to PCRM-associated genes. Orange bars correspond to an overall upregulation of indicated pathways whereas blue is designated for downregulated ones.

References

BERLIVET, S., PAQUETTE, D., DUMOUCHEL, A., LANGLAIS, D., DOSTIE, J. & KMITA, M. 2013. Clustering of tissue-specific sub-TADs accompanies the regulation of HoxA genes in developing limbs. *PLoS Genet,* 9**,** e1004018.

COTNEY, J., LENG, J., YIN, J., REILLY, S. K., DEMARE, L. E., EMERA, D., AYOUB, A. E., RAKIC, P. & NOONAN, J. P. 2013. The evolution of lineage-specific regulatory activities in the human embryonic limb. *Cell,* 154**,** 185-96.

DEMARE, L. E., LENG, J., COTNEY, J., REILLY, S. K., YIN, J., SARRO, R. & NOONAN, J. P. 2013. The genomic landscape of cohesin-associated chromatin interactions. *Genome Res,* 23**,** 1224-34.

FEENSTRA, J. M., KANAYA, K., PIRA, C. U., HOFFMAN, S. E., EPPEY, R. J. & OBERG, K. C. 2012. Detection of genes regulated by Lmx1b during limb dorsalization. *Dev.Growth Differ.,* 54**,** 451-462.

VISEL, A., BLOW, M. J., LI, Z., ZHANG, T., AKIYAMA, J. A., HOLT, A., PLAJZER-FRICK, I., SHOUKRY, M., WRIGHT, C., CHEN, F., AFZAL, V., REN, B., RUBIN, E. M. & PENNACCHIO, L. A. 2009. ChIP-seq accurately predicts tissue-specific activity of enhancers. *Nature.,* 457**,** 854-858.

VISEL, A., MINOVITSKY, S., DUBCHAK, I. & PENNACCHIO, L. A. 2007. VISTA Enhancer Browser--a database of tissue-specific human enhancers. *Nucleic Acids Res,* 35**,** D88-92.